Glycobiology, 2017, vol. 27, no. 5, 457–468
doi: 10.1093/glycob/cwx007
Advance Access Publication Date: 27 February 2017
Original Article

Glycan Recognition

Binding characteristics of galectin-3 fusion proteins

Sophia Böcker and Lothar Elling[1]

Laboratory for Biomaterials, Institute for Biotechnology and Helmholtz-Institute for Biomedical Engineering, RWTH Aachen University, Pauwelsstrasse 20, 52074 Aachen, Germany

[1]To whom correspondence should be addressed: Tel: +49-241-8028350; Fax: +49-241-8022387; e-mail: l.elling@biotec.rwth-aachen.de

Received 12 April 2016; Revised 9 December 2016; Editorial decision 10 January 2017; Accepted 13 January 2017

Abstract

Galectin-3 modulates cell adhesion and signaling events by specific binding and cross-linking galactoside containing carbohydrate ligands. Proteolytic cleavage by metalloproteinases yields in vivo N-terminally truncated galectin-3 still bearing the carbohydrate recognition domain. Truncated galectin-3 has been demonstrated to act in vivo as a negative inhibitor of galectin-3 due to higher affinity for carbohydrate ligands. We here present our studies on a series of 12 human galectin-3 protein constructs. Truncated galectin-3 (Δ1–62 and Δ1–116) and fusions with SNAP-tag and/or yellow fluorescent protein (YFP) display altered binding efficiencies (ratio of maximum binding signal and apparent affinity constant K_d) to asialofetuin (ASF) in solid-phase enzyme-linked immunosorbent assay (ELISA) and surface plasmon resonance (SPR) binding assays. Galectin-3(Δ1–62) and full-length (native) galectin-3 have highest affinity to ASF in ELISA and SPR experiments, respectively, whereas galectin-3(Δ1–116) shows only weak binding. We demonstrate here for the first time that SNAP-tag and YFP fusions of galectin-3 and truncated galectin-3 proteins improve binding efficiencies to ASF. SNAP-tagged galectin-3, galectin-3(Δ1–62) and galectin-3(Δ1–116) are found with significant (3- to 6-fold) higher binding efficiencies in SPR when compared with native galectin-3. Fusion of truncated galectin-3 with YFP renders binding properties similar to native galectin-3, whereas in combination with SNAP-tag improved binding characteristics are obtained. Our results emphasize the importance of the N-terminal domain of human galectin-3 for ligand binding. Most importantly, in combination with fusion proteins suitable for the design of diagnostic and therapeutic tools binding properties can be beneficially tuned. The resulting novel protein tools may be advantageous for potential galectin-3 directed applications in tumor diagnostics and therapy.

Key words: fusion protein, galectin-3, SNAP-tag, truncated galectin-3, yellow fluorescent protein

Introduction

Galectins bind β-galactoside glycan structures and are involved in various biological processes (Barondes et al. 1994; Cooper 2002) such as cell adhesion, inflammation, signaling and tumor progression (Hernandez and Baum 2002; Liu et al. 2002; Almkvist and Karlsson 2004; Liu and Rabinovich 2005; Elola et al. 2007; Rabinovich and Toscano 2009). Galectin-1 and galectin-3 have been demonstrated to trigger tumor angiogenesis by cross-linking of *N*-acetyllactosamine (LacNAc) presenting VEGF receptor 2 and prolonging its cell-surface retention (Markowska et al. 2010; Croci et al. 2014; Funasaka et al. 2014; Stanley 2014). Both galectins are therefore considered as targets for cancer therapy. Furthermore, fusion proteins of these galectins are useful tools to target cell-surface presented poly-LacNAc (Kupper et al. 2013). Fusion

proteins of galectin-3 could be used as imaging and/or drug delivery tool in the context of tumor angiogenesis. However, studies on the binding characteristics of the galectin fusion proteins have to be carried out to evaluate their potential as "theranostic" tools.

Galectin-3 is the only member of the chimeric type galectin family and is composed of three domains: a short N-terminal tail (~20 amino acids), a collagen-like domain cleavable by metalloproteinases (~100 amino acids) and the conserved carbohydrate recognition domain (CRD, ~130 amino acids) (Barondes et al. 1994; Dumic et al. 2006). The N-terminal domain of galectin-3 has been demonstrated to be important for the formation of protein oligomers (Hsu et al. 1992; Kuklinski and Probstmeier 1998; Yang et al. 1998; Ahmad et al. 2004a; Fermino et al. 2011; Lepur et al. 2012). However, also the CRD is discussed to induce self-association (Kuklinski and Probstmeier 1998; Yang et al. 1998; Lepur et al. 2012; Vijayakumar et al. 2013). Specific proteolytic cleavage by matrix-metalloproteinases MMP-2 and -9 at position Ala^{62}-Tyr^{63} results in a 22 kDa galectin, comprised of a truncated collagen-like domain (~50 amino acids) and the CRD (Ochieng et al. 1994; Guévremont et al. 2004). In vivo, this process takes place during tumor progression (Wang et al. 2009). It has been shown that galectin-3C, collagenase truncated galectin-3 (Δ1–107), as well as MMP truncated galectin-3 (Δ1–62) act as a negative inhibitor of galectin-3 displaying higher binding affinity to carbohydrate ligands (Ochieng et al. 1998; Mirandola et al. 2011). In addition, the self-association potential is reduced after MMP treatment (Ochieng et al. 1998; Nangia-Makker et al. 2007). Truncated galectin-3 may therefore inhibit tumor angiogenesis and tumor growth and supports the effect of anti-tumor drugs (John et al. 2003; Mirandola et al. 2011; 2014a). The characterization of truncated galectin-3 is an important step toward understanding galectin-3 mediated biological processes in more detail. However, to the best of our knowledge, a detailed analysis of the binding specificity of truncated galectin-3 has not been investigated, so far.

Fluorescently labeled galectins are of high interest for the evaluation of their binding characteristics (Rapoport et al. 2008; Song et al. 2009; Salomonsson et al. 2010). Labeling is often realized by random chemical modification of galectins (Patnaik et al. 2006; Carlsson et al. 2007; Stowell et al. 2008; Song et al. 2009; Salomonsson et al. 2010), which may affect functional regions. Fusions of galectins with fluorescent proteins like eGFP have been used for detection (Davidson et al. 2006; Delacour et al. 2006; Nakahara et al. 2006; de Melo et al. 2007). However, a comparison with native galectin regarding the binding properties has been rarely performed. Another specific fusion protein is introduced by the SNAP-tag technology. The SNAP-tag is a mutated DNA-repair protein O^6-alkylguanine-DNA alkyltransferase with high affinity for benzylguanine (BG) derivatives offering, e.g., directed immobilization of functional proteins (Kindermann et al. 2003; Engin et al. 2010; Hussain et al. 2011; Recker et al. 2011) or coupling of fluorescent dyes (Keppler et al. 2004; Gronemeyer et al. 2005; Juillerat et al. 2005; Lukinavicius et al. 2015).

We have recently introduced fusion proteins of galectin-1 and galectin-3 with combined N-terminal yellow fluorescent protein (YFP) and SNAP-tag as novel tools in glycobiology (Kupper et al. 2013). The fusion proteins showed similar binding characteristics to the glycoprotein standard asialofetuin (ASF) when compared with nonfused galectins. In flow cytometry experiments we demonstrated specific binding of fluorescent SNAP-tag galectin-3 fusion protein to mesenchymal stem cells. We also proved high binding capacity for glycoproteins in affinity chromatography with the immobilized galectin-3 fusion protein on BG-activated Sepharose beads. We concluded so far that the N-terminal SNAP-YFP fusion does not affect the binding specificity of galectin-3.

Here, we report on the characterization of a toolbox of full-length and truncated galectin-3 fusion proteins. N-terminal His_6-tagged full-length galectin-3 and two truncated versions of galectin-3, galectin-3(Δ1–62) and galectin-3(Δ1–116) were fused to SNAP-tag and/or YFP, respectively. The binding properties of all 12 galectin-3 fusion proteins (Scheme 1) to ASF were evaluated under static and flow conditions using solid-phase enzyme-linked immunosorbent assay (ELISA) and surface plasmon resonance (SPR), respectively. Our results demonstrate different binding properties of the galectin-3 fusion proteins depending on the respective protein truncations and their fusion protein partners.

Results and discussion

Production and characterization of full-length and truncated galectin-3 fusion constructs

Twelve His_6-tagged galectin-3 constructs that differ in their fusion protein partners and truncation were designed (Scheme 1), subsequently produced in *Escherichia coli* Rosetta (DE3) pLysS and purified by immobilized metal ion affinity chromatography (IMAC). The protein constructs were named as depicted in Scheme 1. Protein yields between 2.5 and 19 mg protein per 1 g cells were obtained depending on the fusion protein partners and their truncations

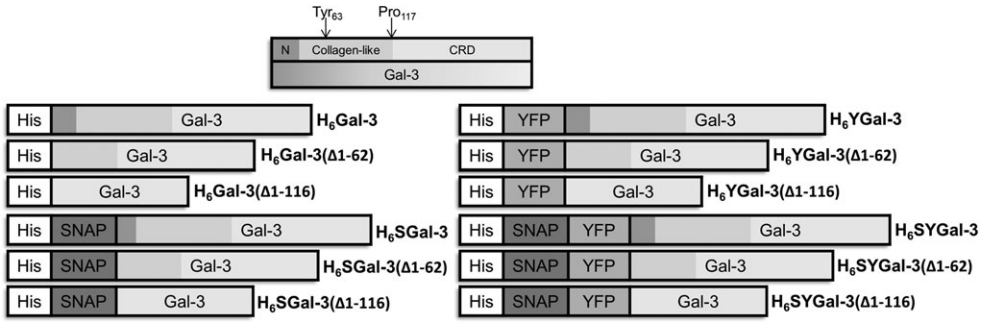

Scheme 1. Protein fusion constructs of human galectin-3. Twelve different Gal-3 fusion proteins were constructed. The constructs differ in the length of the N-terminus and/or type of fusion protein partners. N-terminal His_6-tagged galectin-3 proteins with full-length galectin-3, MMP-derived Δ1–62 truncation of galectin-3 (Gal-3(Δ1–62)) and N-terminal Δ1–116 truncation of galectin-3 (Gal-3(Δ1–116)) were fused to SNAP-tag (S) and/or YFP (Y), respectively. MMP, matrix-metalloproteinases; YFP, yellow fluorescent protein.

(Table I). H_6Gal-3 showed the lowest expression yield, whereas truncation as well as SNAP-tag increased the expression levels.

A second purification step by lactose agarose chromatography was applied to obtain highly purified proteins as analyzed by sodium dodecyl sulfate-polyacrylamide gel electrophoresis (SDS-PAGE; Figure 1A and B) and western blot (Figure 1C and D). Distinct protein bands were detected that fit to the theoretical molecular mass of the corresponding fusion protein (Figure 2 and Supplementary data, Table S1). All proteins detected in the stained gel contained the CRD of galectin-3 that was detected in the western blot by the anti-galectin-3 antibody. Hence, expression and purification of the constructs results in pure proteins of correct sizes. Merely H_6Gal-3 shows an additional band at 29 kDa, which probably indicates cleavage at an additional reported potential cleavage site Gly^{32}-Ala^{33} for collagenases producing a 27 kDa product (Shekhar et al. 2004; Nangia-Makker et al. 2007).

Table I. Yields of galectin-3 fusion proteins after IMAC purification

Protein	Yield (mg/g)	Protein	Yield (mg/g)
H_6Gal-3	2.5	H_6YGal-3	3.5
H_6Gal-3(Δ1–62)	20	H_6YGal-3(Δ1–62)	10
H_6Gal-3(Δ1–116)	17	H_6YGal-3(Δ1–116)	10
H_6SGal-3	9	H_6SYGal-3	12
H_6SGal-3(Δ1–62)	19	H_6SYGal-3(Δ1–62)	17.5
H_6SGal-3(Δ1–116)	16	H_6SYGal-3(Δ1–116)	15.5

Amount of purified galectin-3 fusion proteins is given in mg protein per g cells. IMAC, immobilized metal ion affinity chromatography.

Several functions of galectin-3 are mediated by its oligomerization (Yamaoka et al. 1995; Elola et al. 2007). In former studies, it was shown that truncated galectin-3 (Δ1–62 and Δ1–107) has reduced self-association potential (Kuklinski and Probstmeier 1998; Ochieng et al. 1998). We performed size exclusion chromatography (SEC) to investigate the influence of the SNAP-tag and YFP as well as the truncation on the oligomerization potential of galectin-3 in solution (Supplementary data, Figures S1 and S2).

Figure 2 shows that molecular masses determined by SEC fit well with the theoretical values for all proteins constructs. Moreover, all protein constructs eluted as one peak (Supplementary data, Figure S2). We conclude that neither SNAP-tag nor YFP alter the integrity of the galectin-3 proteins as monomers in solution as described formerly for native human galectin-3 (Hsu et al. 1992; Massa et al. 1993; Ochieng et al. 1993; Morris et al. 2004).

Binding of galectin-3 fusion proteins to ASF in a solid-phase assay

The binding properties of the galectin-3 constructs were tested using the glycoprotein ASF, a suitable ligand for galectin characterization

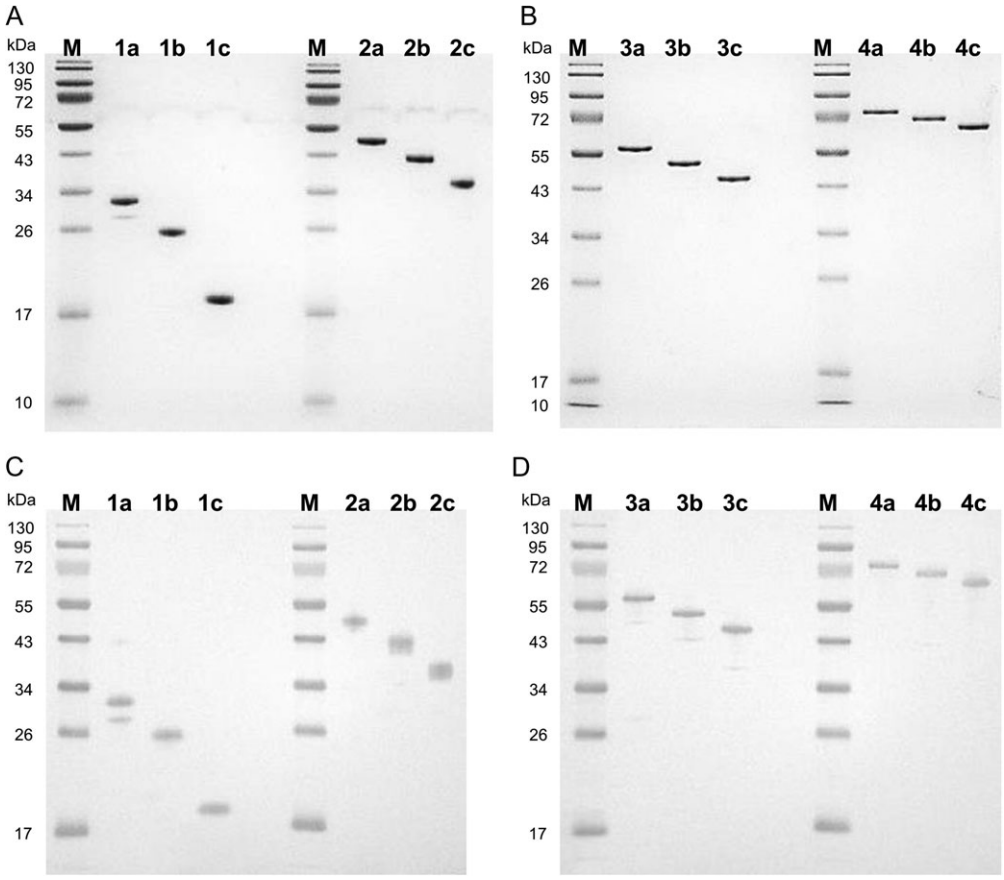

Fig. 1. SDS-PAGE and western blot analysis of purified galectin-3 fusion proteins. The purified galectin-3 fusion proteins were analyzed by SDS-PAGE with subsequent Coomassie-staining (**A**, **B**) and by western blot (**C**, **D**) using an anti-galectin-3 antibody. **M**, Marker; **a**, full-length galectin-3; **b**, galectin-3(Δ1–62); **c**, galectin-3(Δ1–116); **1**, His_6-tag (H_6) fusion; **2**, H_6-SNAP-tag fusion; **3**, H_6-YFP fusion; **4**, H_6-SNAP-tag-YFP fusion. SDS-PAGE, sodium dodecyl sulfate-polyacrylamide gel electrophoresis.

(Sato and Hughes 1992). Figure 3(A–D) depicts the binding curves for each galectin construct. We found that the absolute binding signals of galectin constructs purified by IMAC and by IMAC followed by lactose affinity chromatography are very similar (Supplementary data, Figure S3). We concluded that IMAC purification is sufficient for comparative binding assays of these constructs avoiding also extensive buffer exchange for removal of interfering lactose traces.

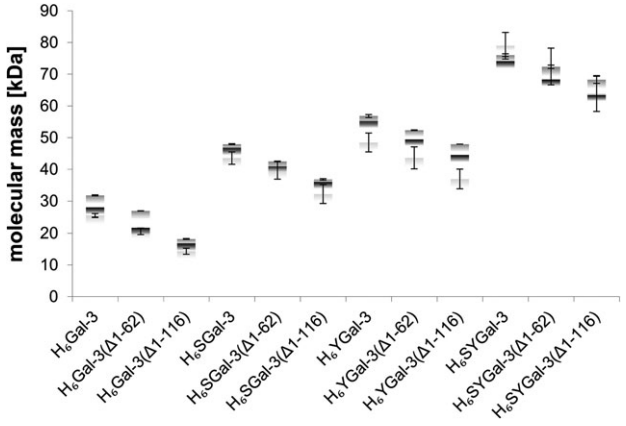

Fig. 2. Comparison of molecular masses of galectin-3 fusion proteins obtained by SDS-PAGE and SEC. Molecular masses of galectin-3 fusion proteins determined by SEC (light gray) and by SDS-PAGE (gray) as well as theoretical molecular masses (black) are given. See Table S1 in supplementary data for molecular mass values. SEC, size exclusion chromatography.

Binding of the His_6-tagged galectin-3 proteins differs significantly depending on the truncation (Figure 3A). Compared to full-length H_6Gal-3, H_6Gal-3(Δ1–62) binds most efficient whereas the H_6Gal-3 (Δ1–116) shows only a weak binding signal (Figure 3A and Supplementary data, Table S2). These differences are also reflected by the calculated apparent K_d values (Figure 4) and binding efficiencies (Table II). The K_d value is the concentration at which 50% saturation of the binding signal is reached and a measure for binding affinity (Hulme and Trevethick 2010; Böcker et al. 2015). Binding efficiency takes the different saturation levels into account by calculating the ratio of maximum binding signals and the apparent K_d values. Among the His_6-tagged constructs, H_6Gal-3(Δ1–62) shows the highest binding affinity to ASF with an apparent K_d value of 4 μM (Figure 4) and a 2-fold increased binding efficiency compared to H_6Gal-3 (Table II). We confirm previously published data demonstrating tight binding of truncated galectin-3(Δ1–62) to immobilized laminin in a similar solid-phase assay (Ochieng et al. 1998). Most interestingly, His_6Gal-3(Δ1–116) lacking the whole N-terminal domain but still presenting the CRD binds only poorly with an almost 10-fold lower binding efficiency compared to H_6Gal-3 (Table II). Our

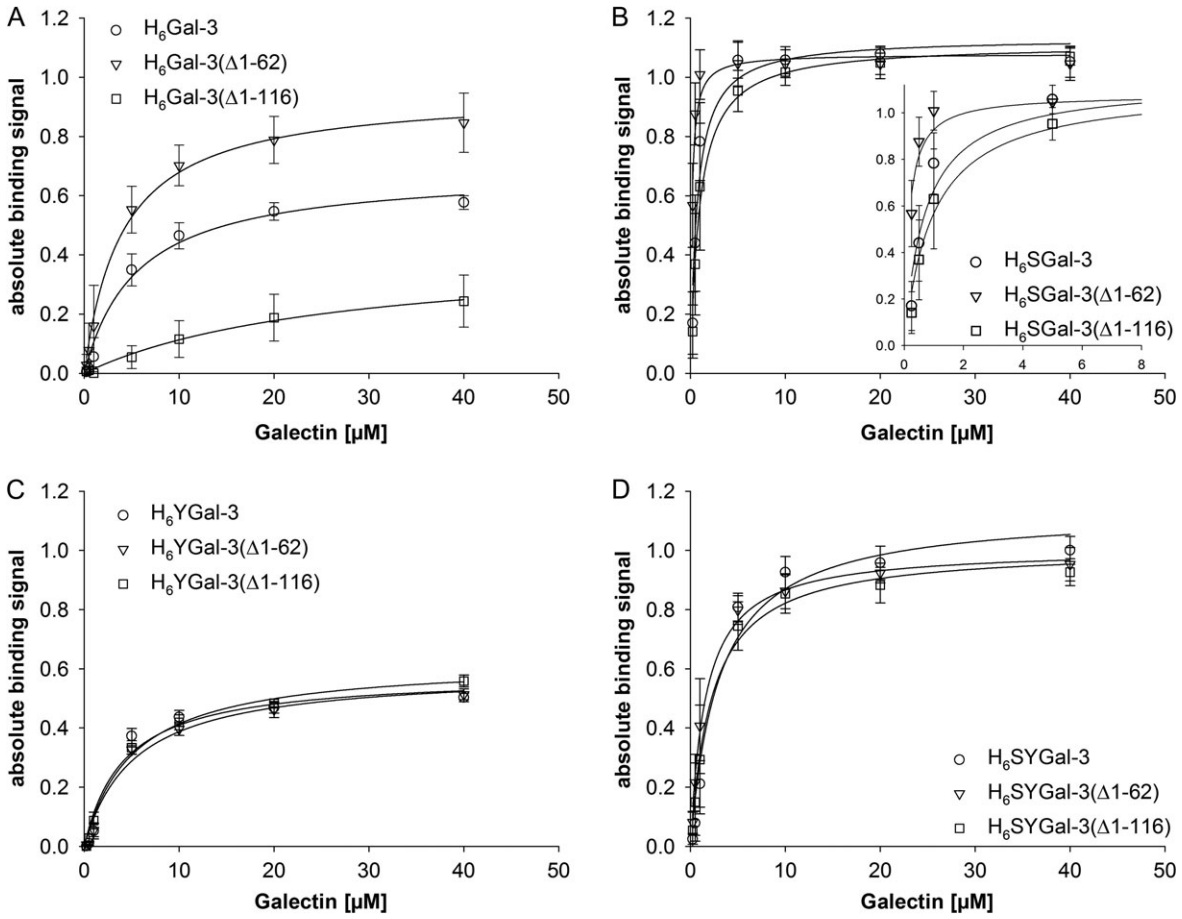

Fig. 3. Binding of galectin-3 protein constructs to ASF in a solid-phase ELISA assay. Absolute binding signals are compared for the different fusion types: His_6-tag (H_6, **A**); H_6-SNAP-tag (H_6S, **B**); H_6-YFP (H_6Y, **C**); H_6-SNAP-tag-YFP (H_6SY, **D**), and truncation types: full-length galectin-3 (circle); galectin-3(Δ1–62) (triangle); galectin-3(Δ1–116) (square). In **B**, binding curves are additionally zoomed for better comparison in the low-concentration range. ASF, asialofetuin; ELISA, enzyme-linked immunosorbent assay.

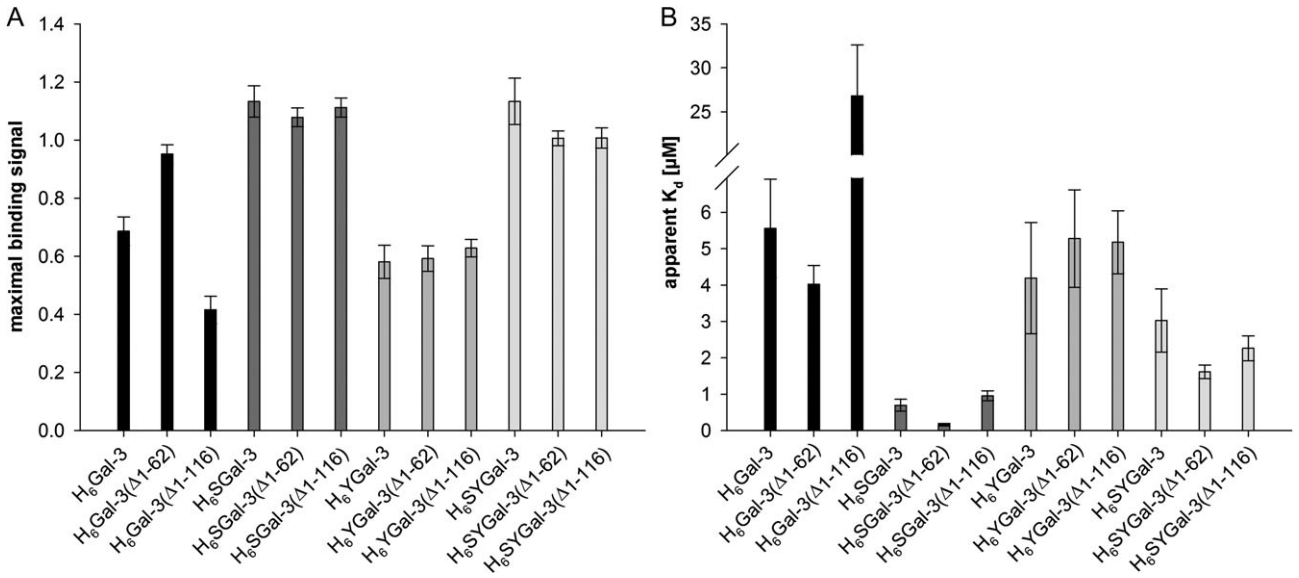

Fig. 4. Calculated maximum binding and apparent K_d values for galectin-3 fusion protein binding to ASF in a solid-phase ELISA assay. For all fusion and truncation variants of galectin-3 values for maximal binding to ASF (**A**) as well as apparent K_d (**B**) are compared. Values were calculated by nonlinear fit of binding data (see Figure 3 and Supplementary data, Table S2).

Table II. Calculated binding efficiencies in ELISA and calculated K_d values in SPR binding experiments to ASF

	ELISA[a]		SPR	
Protein	Binding efficiency (μM^{-1})	Binding potency[b]	Apparent K_d (µM)	Binding potency[c]
H_6Gal-3	0.12 ± 0.05	1.0	32.46 ± 7.40	1.0
H_6Gal-3(Δ1–62)	0.24 ± 0.04	1.9	40.37 ± 9.58	0.8
H_6Gal-3(Δ1–116)	0.02 ± 0.01	0.1	60.02 ± 28.4	0.5
H_6SGal-3	1.62 ± 0.59	13.2	8.56 ± 0.65	3.8
H_6SGal-3(Δ1–62)	6.65 ± 2.11	53.9	10.40 ± 2.13	3.1
H_6SGal-3(Δ1–116)	1.16 ± 0.23	9.4	5.55 ± 1.60	5.8
H_6YGal-3	0.14 ± 0.10	1.1	12.79 ± 0.43	2.5
H_6YGal-3(Δ1–62)	0.11 ± 0.05	0.9	27.01 ± 2.08	1.2
H_6YGal-3(Δ1–116)	0.12 ± 0.03	1.0	37.22 ± 5.42	0.9
H_6SYGal-3	0.37 ± 0.19	3.0	9.89 ± 2.33	3.3
H_6SYGal-3(Δ1–62)	0.62 ± 0.10	5.1	12.92 ± 1.45	2.5
H_6SYGal-3(Δ1–116)	0.45 ± 0.10	3.6	20.29 ± 3.38	1.6

Relative improvement for galectin-3 fusion proteins in comparison to H_6Gal-3 is indicated. ELISA, enzyme-linked immunosorbent assay; SPR, surface plasmon resonance; ASF, asialofetuin.

[a]Since saturation values differ for binding of galectin-3 proteins in ELISA experiments, binding efficiency values were calculated as ratio of maximum binding signal and apparent K_d value (Supplementary data, Table S2). A higher binding efficiency is due to higher maximum binding and/or lower K_d values (app. affinity constant).

[b]Ratio of binding efficiency of Gal-3 construct and binding efficiency of H_6Gal-3

[c]Ratio of app. K_d values of H_6Gal-3 and Gal-3 construct.

results underscore the importance of N-terminal sequences of human galectin-3 for efficient ligand binding. A peptide consisting of amino acids 98–112 of human Gal-3 N-term showed association with the CRD (Berbís et al. 2014) and could probably lead to tight ligand interaction.

N-terminal fusion of the SNAP-tag significantly improves binding of all galectin-3 constructs to ASF (Figure 3 and Table II). Subtle differences among the differently truncated galectin-3 constructs occur at low protein concentrations (Figure 3B, insert). Maximum binding is already reached at protein concentrations below 10 µM with best binding performance of H_6SGal-3(Δ1–62) followed by H_6SGal-3 and H_6SGal-3(Δ1–116). This is also reflected by significantly lower apparent K_d values (Figure 4B) and up to over 50-fold increased binding efficiency when compared with H_6Gal-3 (Table II). Most importantly, complete exchange of the N-terminal domain by the SNAP-tag renders the galectin-3 CRD domain as a fully functional lectin with a 9-fold improved binding efficiency toward ASF. We can conclude that the SNAP-tag fusion is in general beneficial for galectin-3 binding to ASF in a solid-phase ELISA. Fusion with YFP alters the individual binding properties of the galectin-3 constructs as well (Figure 3C). Identical binding curves with similar binding behavior as H_6Gal-3 (Figure 3C and A) are

obtained. Importantly, also YFP fusion improves binding of galectin-3(Δ1–116) resulting in similar maximum binding and K_d values as obtained for full-length galectin-3 (Figure 4 and Supplementary data, Table S2). However, YFP fusion has no effect on the binding properties of full-length galectin-3 (H_6Gal-3 vs. H_6YGal-3) as seen in Figure 4 and Table II. We conclude that N-terminal fusion of YFP to truncated galectin-3 may mimic the natural N-terminal domain of galectin-3 (Scheme 1).

The SNAP-tag-YFP-fusion of galectin-3 combines both effects of each fusion protein (Figure 3D). The binding curves are similar for the full-length and truncated constructs, however, with enhanced binding to ASF. The SNAP-tag increases the binding signal as well as binding affinity, whereas YFP equalizes the influence of truncation yielding overall lower K_d values and higher binding efficiency (Figure 4 and Table II). We can exclude the possibility that the SNAP-tag and YFP were directly involved in binding as a suitable construct, H_6SY lacking complete galectin-3, did not show any binding to ASF (Supplementary data, Figure S4). However, the SNAP-tag could probably be involved in protein oligomerization resulting in higher binding due to detection of complexed SNAP-tagged galectin-3. Oligomerization upon ligand binding is known for galectin-3 (Hsu et al. 1992; Ochieng et al. 1993; Ahmad et al. 2004a) and certainly influences binding assays based on protein detection by ELISA as performed here. Additionally, oligomeric proteins may bind more tightly, whereas more weakly bound galectin-3 constructs are easily removed during washing steps. As the binding capacity to fixed ASF amount should be the same, the required washing procedure between the incubation steps is sufficient to identify binding differences between the fusion proteins.

Inhibition with competing soluble saccharides proves sugar-mediated binding of all galectin-3 constructs to ASF (Supplementary data, Figure S5). All tested constructs are inhibited by LacNAc and Di-LacNAc. As competitive inhibition by the free glycan is investigated, higher competitive inhibitor concentrations were needed to inhibit binding to ASF for galectin-3 constructs with high binding efficiency. Since the affinity of galectin-3 is higher to Di-LacNAc than to the disaccharide LacNAc (Kupper et al. 2013), the inhibition curves for Di-LacNAc in this study are shifted to lower inhibition concentrations. This is the case for all constructs indicating no influence of the fusion partners on the binding specificity. Recently, we proved additionally that H_6SYGal-3 revealed very similar binding specificity even to longer oligosaccharides with up to four LacNAc units compared to H_6Gal-3 (Kupper et al. 2013). Our results confirm a previous study for a alkaline phosphatase/galectin-3 fusion protein showing no difference in binding specificity (de Melo et al. 2007).

In general, we determined apparent K_d values in the area of 10^{-5} to 10^{-7} M which fits well with the reported K_d value (2 μM) for galectin-3 binding to ASF obtained by a titration experiment (von Mach et al. 2014). Truncations as well as fusion protein partners have a significant influence on the K_d values (Figure 4B). The strongest ASF binding could be recorded for H_6SGal-3(Δ1–62) shown by an apparent K_d in the high nanomolar range that is about 35-fold lower than H_6Gal-3. The SNAP-tag may influence the CRD formation and increase the oligomerization potential. Our results confirm previous studies on differences in the binding characteristics of full-length and truncated galectin-3. In vivo, it was shown that MMP-2 cleaved galectin-3 displays 20-fold higher affinity to human umbilical vein endothelial cells (Shekhar et al. 2004). We found a 2-fold higher binding efficiency of H_6Gal-3(Δ1–62) compared to H_6Gal-3 (Table II). The crystal structure of human galectin-3(Δ1–112) reveals optimal binding of lactose, where amino acids 1–112 are not involved (Saraboji et al. 2012). However, as we observe low binding of H_6Gal-3(Δ1–116), it is possible that N-terminally missing amino acids contribute to ligand binding. The four additionally truncated amino acids are just outside the canonical galectin beta-sandwich but they are ordered in crystal structures and might contribute to stability. A previous study with hamster galectin-3 also suggests the involvement of amino acids of the N-terminal domain for binding to the glycoprotein laminin (Barboni et al. 2000). It was shown that truncated galectin-3(Δ1–93) binds stronger to laminin than galectin-3(Δ1–103). Here, Tyr^{102} and adjacent amino acids contribute significantly to oligosaccharide binding. The small N-terminal region was therefore considered to induce a change in CRD structure altering carbohydrate binding specificity.

N-terminal truncation of galectin-3 influences not only binding properties but also other biological functions. Compensation of a missing N-terminal region could also be observed in nuclear localization experiments with hamster and murine galectin-3 (Gaudin et al. 2000; Davidson et al. 2006). It was demonstrated that sequences in the N-terminal domain are important for nuclear localization and diminishes this process after deletion. The important sequences could be substituted by an unrelated sequence, e.g., the fusion with green fluorescent protein and maltose binding protein, leading to similar results for truncated and full-length galectin-3.

SPR spectroscopy of galectin-3 fusion proteins on immobilized ASF

The characteristics of the galectin-3 constructs for ASF binding were also monitored in SPR experiments under flow conditions. The SPR sensor chip is made of a 3D matrix for ligand multilayer immobilization. In detail, ASF was immobilized via the amino groups on a carboxymethyldextran hydrogel chip activated by EDC/Sulfo-NHS. Bovine serum albumin (BSA) was subsequently immobilized on both, sample and reference flow cell. BSA immobilization turned out to be advantageous due to equal protein loads of sample and reference channel and minimized unspecific binding of galectin.

Binding experiments were run with a flow rate of 20 μL/min. Binding curves are shown in Figure 5. They arise from the averaged response at equilibrium of association for seven different galectin-3 concentrations (Supplementary data, Figure S6). The association and dissociation kinetics were quite fast, and dissociation of H_6Gal-3 reached baseline almost completely. This behavior of galectin-3 in SPR experiments was previously reported (Maljaars et al. 2008). Incomplete dissociation was seen for high protein concentrations of fusion proteins with SNAP and YFP (Supplementary data, Figure S6). Calculated maximum binding response and apparent K_d values of the galectin-3 constructs are shown in Figure 6. It should be noted that SPR experiments were performed to investigate the binding behavior of galectin constructs under flow conditions. To maintain highest comparability between ELISA and SPR analysis, we calculated K_d of SPR-experiments not by the kinetic constants k_{on} and k_{off}, but in the same way as mentioned for our ELISA approach, where K_d is the concentration at which 50% saturation of the binding signal is reached. This method was previously used for SPR-based galectin studies (Maljaars et al. 2008).

In contrast to the solid-phase ELISA assay, SPR reveals highest binding for full-length galectin-3 when compared with galectin-3 (Δ1–62) (Figure 5A–C). H_6Gal-3(Δ1–116) binds weakest to ASF as observed in ELISA assay. The binding curve progressions are similar for SNAP-tag and YFP fusion proteins of galectin-3(Δ1–62) and

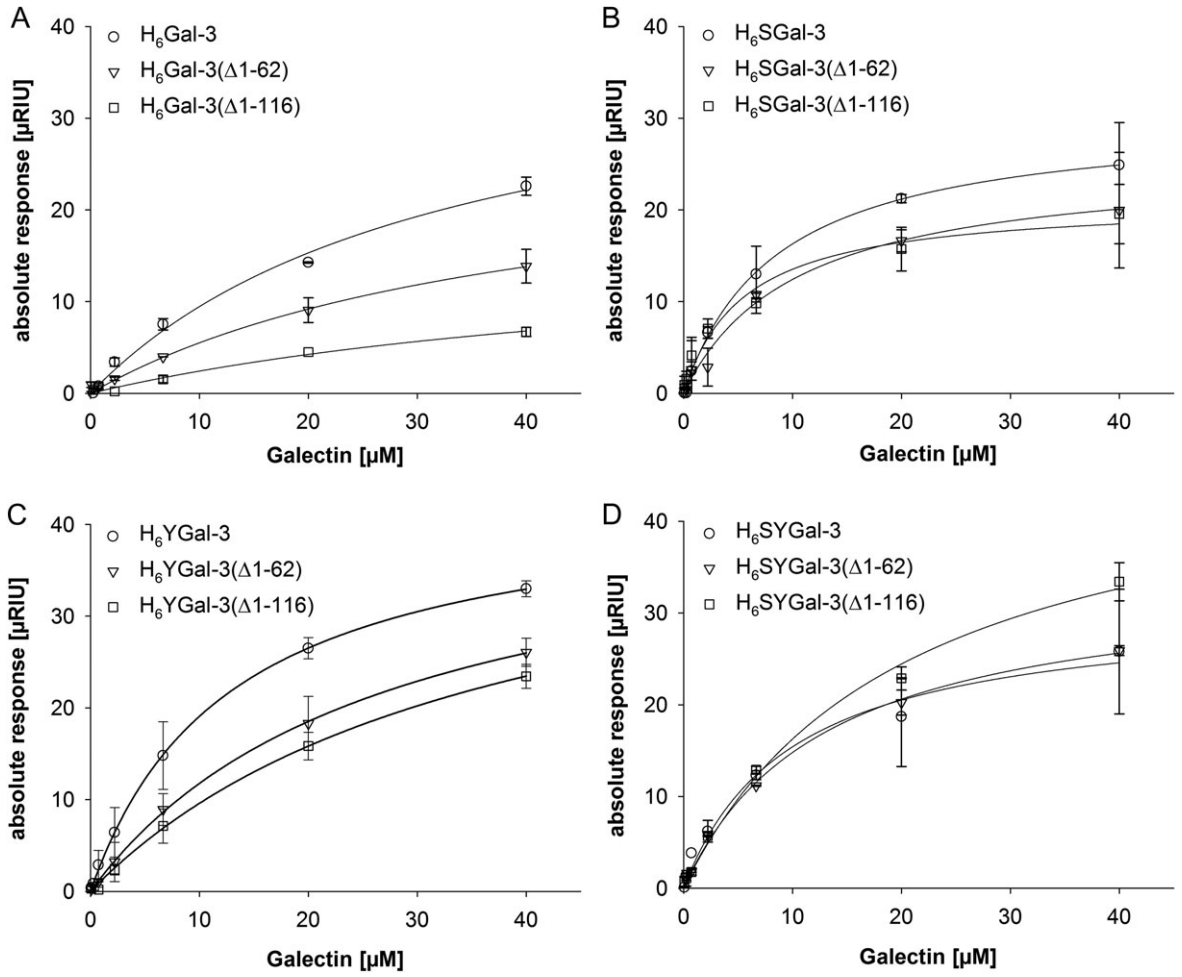

Fig. 5. Binding of galectin-3 fusion proteins to ASF in SPR measurements. Galectin binding to immobilized ASF was monitored under flow (20 µL/min). Binding responses at equilibrium of seven concentrations (0.08–40 µM) of galectin-3 fusion proteins were plotted and fitted by nonlinear regression. Binding curves are shown for the different fusion types: His_6-tag (H_6, **A**); H_6-SNAP-tag (H_6S, **B**); H_6-YFP (H_6Y, **C**); H_6-SNAP-tag-YFP (H_6SY, **D**), and truncation types: full-length galectin-3 (circle); galectin-3(Δ1–62) (triangle); galectin-3(Δ1–116) (square).

galectin-3(Δ1–116) (Figure 5B and C). However, regarding the His_6-YFP and the His_6-SNAP-tag-YFP fusion a different order can be observed. The response of the galectin-3(Δ1–116) reaches the highest values, followed by galectin-3(Δ1–62) and galectin-3 (Figure 6A). It is possible that those constructs with slightly lower molecular mass due to truncation have less steric problems and could reach higher saturation. In contrast, the maximal binding signals for SNAP-tag fusion proteins are in the same range (Figure 6A). To compare maximum binding of proteins with a different size, the signals were normalized by dividing them by the respective molecular mass of the protein. We conclude that, contrary to the solid-phase assay, galectin-3(Δ1–62) shows no dominant binding to ASF in SPR. However, in both flow and solid-phase assays, the N-terminal SNAP-tag and/or YFP fusions render the galectin-3 CRD domain as a fully functional binding domain.

The calculated apparent K_d values (Figure 6B and Table II) further underline the binding differences of the His_6-tagged galectin-3 constructs that are, in contrast, not as distinct as for the solid-phase assay. The SNAP-tag and SNAP-tag-YFP fusions show higher affinity to ASF than the YFP fused variants indicated by lower apparent K_d (Table II). The order of affinity constants for the different fusion types resembles that derived from ELISA assay. However, due to flow conditions in SPR increases of binding efficiencies are lower than those observed in the solid-phase ELISA assay (Table II). Flow makes binding to a ligand more difficult due to shear forces. Under flow conditions, binding behavior of proteins can be different compared to static conditions in solid-phase assays (Campbell et al. 2009; Hu et al. 2013). With ELISA assay the binding efficiency is calculated at binding equilibrium conditions after 1 h incubation time and standardized washing and incubation steps. It is not surprising that under more vigorous flow like in SPR, the K_d values are higher than with static ELISA conditions. Additionally, the different time-course of both experiments leads to different time points for establishing the equilibrium. It has been reported elsewhere that measured values of static assays and flow-assays may differ. An inhibition assay to detect paralytic shellfish poisoning toxins by ELISA and SPR biosensor technology gave lower IC_{50} values under static ELISA conditions (Campbell et al. 2009). Similar results reporting weaker binding under flow conditions were published for a dengue virus immunoassay (Hu et al. 2013).

The lowest apparent K_d values (highest affinity) are reached by SNAP-tag fused galectins, and the lowest affinity by His_6-tagged galectins (Figure 6B and Table II). Most remarkably, in both assays, the H_6SGal-3(Δ1–116) reaches a 6-fold higher affinity for ASF

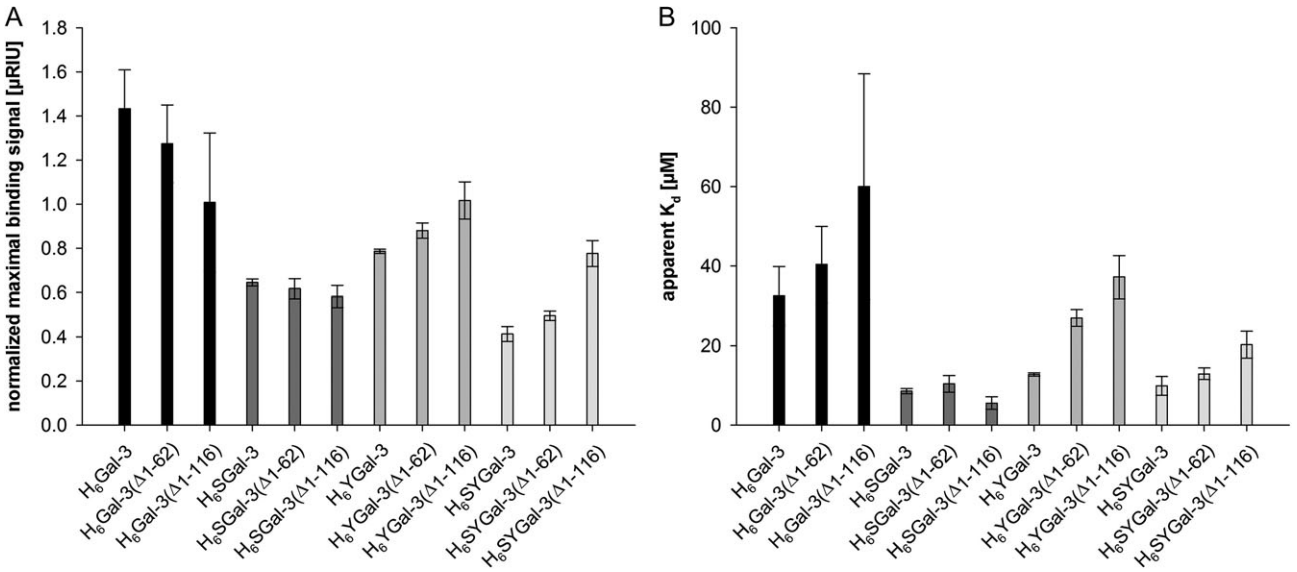

Fig. 6. Calculated values for maximum binding and apparent K_d of galectin-3 protein constructs for binding to ASF in SPR measurements. For all fusion and truncation variants of galectin-3 values for maximal binding to ASF (**A**) as well as apparent K_d (**B**) are compared. Values were calculated by nonlinear fit of binding data (see Figure 5). Normalized maximal binding signals were obtained after division of the absolute maximal response signal by the molecular mass of the corresponding galectin-3 protein construct.

when compared with H_6Gal-3 (Table II). The apparent K_d for H_6Gal-3 of ~32 µM (Table II) is in good accordance to the reported K_d of 21.5 µM for human galectin-3 in a similar experimental setup (Maljaars et al. 2008). The general higher binding efficiency of galectin-3(Δ1–62) constructs compared to full-length galectin-3 could not be seen in SPR under flow conditions (Table II). Although several studies showed better binding of truncated galectin-3 (Ochieng et al. 1998; Shekhar et al. 2004), isothermal titration calorimetry revealed similar affinity constants for full-length and truncated galectin-3 (Ahmad et al. 2004b; Yegorova et al. 2013) or even contradictory results where doubled association constant was measured for galectin-3 compared to truncated galectin-3 (Dam et al. 2005).

In summary, similar conclusions can be drawn from our SPR experiments: N-terminal fusions of SNAP-tag to full-length and truncated galectin-3 (Δ1–62 and Δ1–116) as well as to YFP-fusion proteins thereof improve binding to ASF. In addition, SNAP-tag and/or YFP fusions promote the binding affinity of galectin-3(Δ1–116).

With their enhanced affinity SNAP-tagged Gal-3 fusion proteins could be candidates for anti-tumor therapy and may also serve as novel tools in molecular imaging. The SNAP-tag offers coupling of drugs or fluorescent dyes and other reporter groups and therefore easy localization of galectin-3 in vivo. Truncated galectin-3 is present in tumor where competition with endogenous galectin-3 could lead to reduced tumor angiogenesis, metastasis and progression (Shekhar et al. 2004; Jarvis et al. 2012). Therapy approaches using exogenous truncated galectin-3 to decrease tumor volumes and metastases were already successful in mouse models of breast cancer, multiple myeloma and ovarian cancer (John et al. 2003; Mirandola et al. 2011, 2014a, 2014b).

Conclusions

The present work demonstrates for the first time the influences of truncations and fusion protein partners on the binding behavior of human galectin-3. Our results confirm in agreement to literature a higher affinity of galectin-3(Δ1–62) toward ASF compared to full-length galectin-3 in solid-phase assay. In contrast, under flow condition full-length galectin-3 depicted highest ASF affinity. Galectin-3 fusion proteins with SNAP-tag achieved increased binding efficiency and binding affinity toward ASF. YFP as fusion protein partner equalizes the influence of galectin-3 truncations. We conclude that sequences in the N-terminal domain are important for ligand detection but can be replaced by an unrelated sequence, here provided by the corresponding fusion proteins. Additionally, it is interesting to note that binding characteristics of galectin-3 fusion proteins are strongly dependent on static or flow conditions in binding assays. This has to be taken into account for galectin-based "theranostics" (e.g., targeting in the blood stream) and their mode of application. This study thus demonstrates how galectin-3 and especially galectin-3(Δ1–62) as well as galectin-3(Δ1–116) are influenced by fusions and can be beneficially tuned for higher binding affinity, being in future advantageous in potential applications for tumor therapy and diagnostics.

Materials and methods

Cloning of galectin constructs

All full-length and truncated galectin-3 constructs for this study have been designed based on the pETDuet-1-vector encoding H_6Gal-3 and the pET17b-vector encoding H_6SYGal-3 (Kupper et al. 2013). For the truncations of galectin-3, we followed on the one hand the main cleavage site of the metalloproteinases MMP-2 and -9 between Ala^{62}-Tyr^{63} (galectin-3(Δ1–62)) and on the other hand the truncation of the entire N-terminal and collagen-like domain until Pro^{117} (galectin-3(Δ1–116)). The genes for galectin-3(Δ1–62) and galectin-3(Δ1–116) were amplified from pETDuet-H_6Gal-3 and the restriction sites for *Eco*RI and *Not*I were simultaneously introduced using the primers 5′-AAGAA TTCAA TGTAC CCTGG AGCAC CTGG-3′ and 5′-TTTGC GGCCG CTTAT ATCAT GGTAT ATGAA GCACT GGTG-3′ for H_6Gal-3(Δ1–62) and

5′-AAGAA TTCAA TGCCT TATAA CCTGC CTTTG CC-3′ and 5′-TTTGC GGCCG CTTAT ATCAT GGTAT ATGAA GCACT GGTG-3′ for H_6Gal-3(Δ1–116). After cutting the pETDuet-H_6Gal-3 and the PCR products with *Eco*RI and *Not*I, the final vectors pETDuet-H_6Gal-3(Δ1–62) and -H_6Gal-3(Δ1–116) were ligated.

The cloning of the galectin-3 fusion proteins with SNAP-tag and YFP was very similar. Amplification and insertion of the restriction sites for *Bsr*GI and *Not*I were done using the primers 5′-ACATG TACAA AATGT ACCCT GGAGC ACCTG G-3′ and 5′-TTTGC GGCCG CTTAT ATCAT GGTAT ATGAA GCACT GGTG-3′ for H_6SYGal-3(Δ1–62) and 5′-ACATG TACAA AATGC CTTAT AACCT GCCTT TGCC-3′ and 5′-TTTGC GGCCG CTTAT ATCAT GGTAT ATGAA GCACT GGTG-3′ for H_6SYGal-3(Δ1–116). Afterwards, the restricted pET17b-H_6SYGal-3 and the particular PCR product were ligated to pET17b-H_6SYGal-3(Δ1–62) and -H_6SYGal-3 (Δ1–116).

The SNAP-tag fusion constructs H_6SGal-3, H_6SGal-3(Δ1–62) and H_6SGal-3(Δ1–116) were cloned via restriction of pET17b-H_6SYGal-3, -H_6SYGal-3(Δ1–62) and -H_6SYGal-3(Δ1–116), respectively, with *Age*I and *Bsr*GI to remove YFP-gene, Klenow fill-in of the sticky ends and subsequent blunt-end ligation of the vectors.

To generate YFP fusion constructs, the genes for YFP-Gal-3, YFP-Gal-3(Δ1–162) and YFP-Gal-3(Δ1–116) with restriction sites for *Nde*I and *Not*I were amplified from pET17b-H_6SYGal-3, pET17b-H_6SYGal-3(Δ1–62) and pET17b-H_6SYGal-3(Δ1–116), respectively, using the primers 5′-AAAAA ACATA TGGTG AGCAA GGGC-3′and 5′-TTTGC GGCCG CTTAT ATCAT GGTAT ATGAA GCACT GGTG-3′. After restriction of pET28a-vector and PCR products, both were ligated resulting in pET28a-H_6YGal-3, -H_6YGal-3(Δ1–62) and -H_6YGal-3(Δ1–116). All ligation products were transformed in competent cells either *E. coli* NovaBlue (Novagen/Merck, Darmstadt, Germany) or *E. coli* NEB Turbo (NEB, Frankfurt/Main, Germany) for plasmid selection and isolation. Successful cloning was confirmed by sequencing.

Expression and purification

All galectin-3 fusion proteins were expressed in *E. coli* Rosetta (DE3) pLysS (Novagen/Merck, Darmstadt, Germany). Cell cultivation, disruption and protein purification by IMAC (HisTrap™, GE-Healthcare, Munich, Germany) were performed as described elsewhere (Böcker et al. 2015). His_6-tagged and SNAP-tagged galectin-3 constructs were stored in phosphate-buffered saline containing 2 mM EDTA (EPBS, pH 7.5) at 4°C, while YFP as well as SNAP-YFP galectin-3 constructs were frozen in EPBS at −20°C. Buffer exchange was achieved by ultrafiltration (Amicon® Ultra-15, Merck Millipore, Darmstadt, Germany). Protein concentrations were determined by Bradford assay (Roti®-Quant, Carl Roth, Karlsruhe, Germany) using BSA for calibration.

As second purification step affinity chromatography on α-Lactose-Agarose (Sigma-Aldrich, Taufkirchen, Germany) was performed using EPBS as running buffer. A 5–10 mg IMAC-purified protein in EPBS were concentrated by ultrafiltration (Amicon® Ultra-15) and loaded onto Lactose-Agarose, washed and eluted with 200 mM lactose.

SDS-PAGE and western blot

The purification and the size of the purified proteins were checked by SDS-PAGE followed by western blot. Here, 0.4 µg for Coomassie-staining and 0.08 µg for western blot were applied. The proteins transferred to the PVDF-membrane were detected by incubation with anti-galectin-3 antibody (Gal379, Biolegend, Fell, Germany) as primary antibody followed by incubation with anti-mouse-peroxidase (Sigma-Aldrich).

Size exclusion chromatography

Double purified proteins were analyzed by SEC using TSK-GEL® $G3000SW_{XL}$ column (5 µm, 7.8 mm ID × 30.0 cm *L*, 10–500 kDa (globular proteins), Tosoh bioscience, Stuttgart, Germany). About 0.2 nmol protein in 20 µL EPBS was applied onto the column with a flow rate of 0.5 mL/min. The buffer consisting of 0.05 M phosphate, 0.15 M NaCl, pH 7 was used for protein elution. For molecular mass calculation, different calibration standards (Serva, Heidelberg, Germany and Bio-Rad, Munich, Germany) were used (Supplementary data, Figure S1).

Galectin binding assay on ASF

Binding of full-length and truncated galectin-3 fusion proteins to ASF (Sigma-Aldrich) was analyzed by an ELISA type assay in 96-well microtiter plate format as previously described (Kupper et al. 2013). Briefly, ASF (200 µL of 5 µg/mL bovine ASF in sodium carbonate buffer pH 9.6) was immobilized in microtiter plates (MaxiSorp, Nunc, Wiesbaden, Germany) over night. After blocking of residual binding sites with BSA (2% in PBS) different amounts of galectin were incubated for 1 h in EPBS. Three times washing was done with 250 µL PBS containing 0.05% Tween® 20 (AppliChem, Darmstadt, Germany) between the incubation steps. Bound galectin was detected by incubation with anti-His_6-peroxidase (Roche, Basel, Switzerland, 1:1000 in PBS) and subsequent conversion of *o*-phenylenediamine (OPD, Dako, Hamburg, Germany) with read-out at 492 nm. The presented data are the results of at least three independent measurements. K_d and the maximuml binding response were calculated for each galectin-3 fusion construct by nonlinear fitting (ligand binding model: $y = \frac{B_{max} \cdot x}{K_d + x}$, SigmaPlot (Systat, Erkrath, Germany)). K_d is the concentration at half-maximum binding signal.

Inhibition of galectin binding with (Di-)LacNAc-linker-*t*Boc

Specific binding of the full-length and truncated galectin-3 constructs was proved by two oligosaccharides used for competitive inhibition studies of galectin-ASF binding. LacNAc-linker-*t*Boc (LacNAc) and Di-LacNAc-linker-*t*Boc (Di-LacNAc) were synthesized and purified as described previously (Sauerzapfe et al. 2009; Rech et al. 2011; Böcker et al. 2015). After immobilization of ASF and blocking as described before, different concentrations of saccharide were simultaneously incubated with galectin for 1 h in EPBS. Controls without glycan and without galectin were performed to indicate minimal and maximal binding, respectively. Residual bound galectin was detected as described by anti-His_6-peroxidase and OPD conversion. All assays were reproduced in at least three independent measurements.

SPR spectroscopy

SPR spectroscopy was performed with Reichert SR7500DC System (XanTec, Düsseldorf, Germany) using carboxymethyldextran hydrogel sensor chips (200 M, XanTec). ASF was immobilized on a chip via EDC-Sulfo-NHS coupling. The immobilization was carried out with a flow rate of 10 µL/min. After activating the surface with 40 µL Sulfo-NHS/EDC in 100 mM MES 10 µL ASF (5 µg/mL in 10 mM acetate buffer, pH 4.5) was applied on the sample channel. To get similar surface condition for sample and reference both flow

cells were treated with 2% BSA for 2 min. Remaining NHS esters were blocked by injecting 1 M ethanolamine (60 µL, pH 8.5).

The binding experiments were carried out with a flow rate of 20 µL/min by successively injecting seven different galectin concentrations in EPBS from low to high concentration (0.08 to 40 µM). The dissociation time was 3 min. Between the measurements of different galectin-3 fusion proteins the surface was regenerated several times with 1 M NaCl/20 mM HCl and 500 mM lactose.

The measured data were subtracted by reference and blank values using Scrubber2 (BioLogic Software, Campbell, Australia). The averaged binding response values for each concentration at the equilibrium binding (average responses from 60 to 140 s) of two different measurements were plotted against the galectin concentration and K_d and the maximal binding response were calculated for each galectin-3 fusion construct by nonlinear fitting (ligand binding model: $y = \frac{B_{max} \bullet x}{K_d + x}$, SigmaPlot (Systat, Erkrath, Germany)). The maximal binding signals were normalized to the molecular mass of the corresponding protein construct dividing by the corresponding molecular masses (Figure 6).

Supplementary data

Supplementary data are available at *Glycobiology* online.

Acknowledgements

We thank Dr. Andreas Walther and Prof. Dr. Martin Möller (DWI Leibniz Institute for Interactive Materials, Aachen) for the opportunity to perform measurements using the SPR device.

Funding

"Deutsche Forschungsgemeinschaft" (DFG) within the Research Training Group "GRK 1035: Biointerface – Detection and Control of Interface-induced Biomolecular and Cellular Functions".

Conflict of interest statement

None declared.

Abbreviations

ASF, asialofetuin; BG, benzylguanine; BSA, bovine serum albumin; CRD, carbohydrate recognition domain; EDC, 1-ethyl-3-(3-dimethylaminopropyl)-carbodiimide; EDTA, ethylenediamine tetraacetic acid; ELISA, enzyme-linked immunosorbent assay; EPBS, EDTA-containing PBS; Gal-3, galectin-3; H_6, His_6-tag; IMAC, immobilized metal ion affinity chromatography; LacNAc, *N*-acetyllactosamine; MMP, matrix-metalloproteinases; OPD, *o*-phenylenediamine; PBS, phosphate-buffered saline; SDS-PAGE, sodium dodecyl sulfate-polyacrylamide gel electrophoresis; SEC, size exclusion chromatography; Sulfo-NHS, sulfo-*N*-hydroxysuccinimide; SPR, surface plasmon resonance; YFP, yellow fluorescent protein.

References

Ahmad N, Gabius HJ, André S, Kaltner H, Sabesan S, Roy R, Liu BC, Macaluso F, Brewer CF. 2004a. Galectin-3 precipitates as a pentamer with synthetic multivalent carbohydrates and forms heterogeneous cross-linked complexes. *J Biol Chem*. 279:10841–10847.

Ahmad N, Gabius HJ, Sabesan S, Oscarson S, Brewer CF. 2004b. Thermodynamic binding studies of bivalent oligosaccharides to galectin-1, galectin-3, and the carbohydrate recognition domain of galectin-3. *Glycobiology*. 14:817–825.

Almkvist J, Karlsson A. 2004. Galectins as inflammatory mediators. *Glycoconj J*. 19:575–581.

Barboni EAM, Bawumia S, Henrick K, Hughes RC. 2000. Molecular modeling and mutagenesis studies of the N-terminal domains of galectin-3: Evidence for participation with the C-terminal carbohydrate recognition domain in oligosaccharide binding. *Glycobiology*. 10:1201–1208.

Barondes SH, Cooper DN, Gitt MA, Leffler H. 1994. Galectins. Structure and function of a large family of animal lectins. *J Biol Chem*. 269:20807–20810.

Berbís MA, André S, Canada FJ, Pipkorn R, Ippel H, Mayo KH, Kubler D, Gabius HJ, Jimenez-Barbero J. 2014. Peptides derived from human galectin-3 N-terminal tail interact with its carbohydrate recognition domain in a phosphorylation-dependent manner. *Biochem Biophys Res Commun*. 443:126–131.

Böcker S, Laaf D, Elling L. 2015. Galectin binding to neo-glycoproteins: LacDiNAc conjugated BSA as ligand for human galectin-3. *Biomolecules*. 5:1671–1696.

Campbell K, Huet AC, Charlier C, Higgins C, Delahaut P, Elliott CT. 2009. Comparison of ELISA and SPR biosensor technology for the detection of paralytic shellfish poisoning toxins. *J Chromatogr B Analyt Technol Biomed Life Sci*. 877:4079–4089.

Carlsson S, Oberg CT, Carlsson MC, Sundin A, Niisson UJ, Smith D, Cummings RD, Almkvist J, Karlsson A, Leffler H. 2007. Affinity of galectin-8 and its carbohydrate recognition domains for ligands in solution and at the cell surface. *Glycobiology*. 17:663–676.

Cooper DN. 2002. Galectinomics: Finding themes in complexity. *Biochim Biophys Acta*. 1572:209–231.

Croci DO, Cerliani JP, Dalotto-Moreno T, Méndez-Huergo SP, Mascanfroni ID, Dergan-Dylon S, Toscano MA, Caramelo JJ, García-Vallejo JJ, Ouyang J et al. 2014. Glycosylation-dependent lectin-receptor interactions preserve angiogenesis in anti-VEGF refractory tumors. *Cell*. 156: 744–758.

Dam TK, Gabius H-J, André S, Kaltner H, Lensch M, Brewer CF. 2005. Galectins bind to the multivalent glycoprotein asialofetuin with enhanced affinities and a gradient of decreasing binding constants. *Biochemistry*. 44:12564–12571.

Davidson PJ, Li SY, Lohse AG, Vandergaast R, Verde E, Pearson A, Patterson RJ, Wang JL, Arnoys EJ. 2006. Transport of galectin-3 between the nucleus and cytoplasm. I. Conditions and signals for nuclear import. *Glycobiology*. 16:602–611.

de Melo FHM, Butera D, Medeiros RS, Andrade LND, Nonogaki S, Soares FA, Alvarez RA, Moura da Silva AM, Chammas R. 2007. Biological applications of a chimeric probe for the assessment of galectin-3 ligands. *J Histochem Cytochem*. 55:1015–1026.

Delacour D, Cramm-Behrens CI, Drobecq H, Le Bivic A, Naim HY, Jacob R. 2006. Requirement for galectin-3 in apical protein sorting. *Curr Biol*. 16: 408–414.

Dumic J, Dabelic S, Flögel M. 2006. Galectin-3: An open-ended story. *BBA-Gen Subjects*. 1760:616–635.

Elola MT, Wolfenstein-Todel C, Troncoso MF, Vasta GR, Rabinovich GA. 2007. Galectins: Matricellular glycan-binding proteins linking cell adhesion, migration, and survival. *Cell Mol Life Sci*. 64:1679–1700.

Engin S, Trouillet V, Franz CM, Welle A, Bruns M, Wedlich D. 2010. Benzylguanine thiol self-assembled mono layers for the immobilization of SNAP-tag proteins on microcontact-printed surface structures. *Langmuir*. 26:6097–6101.

Fermino ML, Polli CD, Toledo KA, Liu FT, Hsu DK, Roque-Barreira MC, Pereira-da-Silva G, Bernardes ES, Halbwachs-Mecarelli L. 2011. LPS-induced galectin-3 oligomerization results in enhancement of neutrophil activation. *PLoS ONE*. 6:e26004.

Funasaka T, Raz A, Nangia-Makker P. 2014. Galectin-3 in angiogenesis and metastasis. *Glycobiology*. 24:886–891.

Gaudin JC, Mehul B, Hughes RC. 2000. Nuclear localisation of wild type and mutant galectin-3 in transfected cells. *Biol Cell*. 92:49–58.

Gronemeyer T, Godin G, Johnsson K. 2005. Adding value to fusion proteins through covalent labelling. *Curr Opin Biotechnol*. 16:453–458.

Guévremont M, Martel-Pelletier J, Boileau C, Liu FT, Richard M, Fernandes JC, Pelletier JP, Reboul P. 2004. Galectin-3 surface expression on human

adult chondrocytes: A potential substrate for collagenase-3. *Ann Rheum Dis*. 63:636–643.

Hernandez JD, Baum LG. 2002. Ah, sweet mystery of death! Galectins and control of cell fate. *Glycobiology*. 12:127R–136R.

Hsu DK, Zuberi RI, Liu FT. 1992. Biochemical and biophysical characterization of human recombinant IgE-binding protein, an S-type animal lectin. *J Biol Chem*. 267:14167–14174.

Hu D, Fry SR, Huang JX, Ding X, Qiu L, Pan Y, Chen Y, Jin J, McElnea C, Buechler J et al. 2013. Comparison of surface plasmon resonance, resonant waveguide grating biosensing and enzyme linked immunosorbent assay (ELISA) in the evaluation of a dengue virus immunoassay. *Biosensors*. 3:297–311.

Hulme EC, Trevethick MA. 2010. Ligand binding assays at equilibrium: Validation and interpretation. *Br J Pharmacol*. 161:1219–1237.

Hussain AF, Kampmeier F, von Felbert V, Merk HF, Tur MK, Barth S. 2011. SNAP-tag technology mediates site specific conjugation of antibody fragments with a photosensitizer and improves target specific phototoxicity in tumor cells. *Bioconjug Chem*. 22:2487–2495.

Jarvis GA, Mirandola L, Yuefei Y, Cobos E, Chiriva-Internati M, John CM. 2012. Galectin-3 C: Human lectin for treatment of cancer. In: Klyosov AA, Traber PG, editors. *Galectins and Disease Implications for Targeted Therapeutics*, ACS Symposium Series Vol. 1115, Washington DC: American Chemical Society, p.195–232.

John CM, Leffler H, Kahl-Knutsson B, Svensson I, Jarvis GA. 2003. Truncated galectin-3 inhibits tumor growth and metastasis in orthotopic nude mouse model of human breast cancer. *Clin Cancer Res*. 9:2374–2383.

Juillerat A, Heinis C, Sielaff I, Barnikow J, Jaccard H, Kunz B, Terskikh A, Johnsson K. 2005. Engineering substrate specificity of O6-alkylguanine-DNA alkyltransferase for specific protein labeling in living cells. *ChemBioChem*. 6:1263–1269.

Keppler A, Pick H, Arrivoli C, Vogel H, Johnsson K. 2004. Labeling of fusion proteins with synthetic fluorophores in live cells. *Proc Natl Acad Sci USA*. 101:9955–9959.

Kindermann M, George N, Johnsson N, Johnsson K. 2003. Covalent and selective immobilization of fusion proteins. *J Am Chem Soc*. 125:7810–7811.

Kuklinski S, Probstmeier R. 1998. Homophilic binding properties of galectin-3: Involvement of the carbohydrate recognition domain. *J Neurochem*. 70:814–823.

Kupper CE, Böcker S, Liu HL, Adamzyk C, van de Kamp J, Recker T, Lethaus B, Jahnen-Dechent W, Neuss S, Müller-Newen G et al. 2013. Fluorescent SNAP-tag galectin fusion proteins as novel tools in glycobiology. *Curr Pharm Des*. 19:5457–5467.

Lepur A, Salomonsson E, Nilsson UJ, Leffler H. 2012. Ligand induced galectin-3 protein self-association. *J Biol Chem*. 287:21751–21756.

Liu FT, Patterson RJ, Wang JL. 2002. Intracellular functions of galectins. *BBA-Gen Subjects*. 1572:263–273.

Liu FT, Rabinovich GA. 2005. Galectins as modulators of tumour progression. *Nat Rev Cancer*. 5:29–41.

Lukinavicius G, Reymond L, Johnsson K. 2015. Fluorescent labeling of SNAP-tagged proteins in cells. *Methods Mol Biol*. 1266:107–118.

Maljaars CEP, André S, Halkes KM, Gabius HJ, Kamerling JP. 2008. Assessing the inhibitory potency of galectin ligands identified from combinatorial (glyco)peptide libraries using surface plasmon resonance spectroscopy. *Anal Biochem*. 378:190–196.

Markowska AI, Liu FT, Panjwani N. 2010. Galectin-3 is an important mediator of VEGF- and bFGF-mediated angiogenic response. *J Exp Med*. 207: 1981–1993.

Massa SM, Cooper DNW, Leffler H, Barondes SH. 1993. L-29, an endogenous lectin, binds to glycoconjugate ligands with positive cooperativity. *Biochemistry*. 32:260–267.

Mirandola L, Nguyen DD, Rahman RL, Grizzi F, Yuefei Y, Figueroa JA, Jenkins MR, Cobos E, Chiriva-Internati M. 2014a. Anti-galectin-3 therapy: a new chance for multiple myeloma and ovarian cancer? *Int Rev Immunol*. 33:417–427.

Mirandola L, Yu Y, Cannon MJ, Jenkins MR, Rahman RL, Nguyen DD, Grizzi F, Cobos E, Figueroa JA, Chiriva-Internati M. 2014b. Galectin-3 inhibition suppresses drug resistance, motility, invasion and angiogenic potential in ovarian cancer. *Gynecol Oncol*. 135:573–579.

Mirandola L, Yu YF, Chui K, Jenkins MR, Cobos E, John CM, Chiriva-Internati M. 2011. Galectin-3 C inhibits tumor growth and increases the anticancer activity of bortezomib in a murine model of human multiple myeloma. *PLoS One*. 6:e21811.

Morris S, Ahmad N, Andre S, Kaltner H, Gabius HJ, Brenowitz M, Brewer F. 2004. Quaternary solution structures of galectins-1, -3, and -7. *Glycobiology*. 14:293–300.

Nakahara S, Oka N, Wang Y, Hogan V, Inohara H, Raz A. 2006. Characterization of the nuclear import pathways of galectin-3. *Cancer Res*. 66:9995–10006.

Nangia-Makker P, Raz T, Tait L, Hogan V, Fridman R, Raz A. 2007. Galectin-3 cleavage: A novel surrogate marker for matrix metalloproteinase activity in growing breast cancers. *Cancer Res*. 67:11760–11768.

Ochieng J, Fridman R, Nangiamakker P, Kleiner DE, Liotta LA, Stetlerstevenson WG, Raz A. 1994. Galectin-3 is a novel substrate for human matrix metalloproteinases-2 and -9. *Biochemistry*. 33:14109–14114.

Ochieng J, Green B, Evans S, James O, Warfield P. 1998. Modulation of the biological functions of galectin-3 by matrix metalloproteinases. *BBA-Gen Subjects*. 1379:97–106.

Ochieng J, Platt D, Tait L, Hogan V, Raz T, Carmi P, Raz A. 1993. Structure-function relationship of a recombinant human galactoside-binding protein. *Biochemistry*. 32:4455–4460.

Patnaik SK, Potvin B, Carlsson S, Sturm D, Leffler H, Stanley P. 2006. Complex N-glycans are the major ligands for galectin-1, -3, and -8 on Chinese hamster ovary cells. *Glycobiology*. 16:305–317.

Rabinovich GA, Toscano MA. 2009. Turning 'sweet' on immunity: Galectin-glycan interactions in immune tolerance and inflammation. *Nat Rev Immunol*. 9:338–352.

Rapoport EM, André S, Kurmyshkina OV, Pochechueva TV, Severov VV, Pazynina GV, Gabius HJ, Bovin NV. 2008. Galectin-loaded cells as a platform for the profiling of lectin specificity by fluorescent neoglycoconjugates: A case study on galectins-1 and-3 and the impact of assay setting. *Glycobiology*. 18:315–324.

Rech C, Rosencrantz RR, Křenek K, Pelantová H, Bojarová P, Römer CE, Hanisch F-G, Křen V, Elling L. 2011. Combinatorial one-pot synthesis of poly-*N*-acetyllactosamine oligosaccharides with leloir-glycosyltransferases. *Adv Synth Catal*. 353:2492–2500.

Recker T, Haamann D, Schmitt A, Kuster A, Klee D, Barth S, Müller-Newen G. 2011. Directed covalent immobilization of fluorescently labeled cytokines. *Bioconjug Chem*. 22:1210–1220.

Salomonsson E, Carlsson MC, Osla V, Hendus-Altenburger R, Kahl-Knutson B, Oberg CT, Sundin A, Nilsson R, Nordberg-Karlsson E, Nilsson UJ et al. 2010. Mutational tuning of galectin-3 specificity and biological function. *J Biol Chem*. 285:35079–35091.

Saraboji K, Hakansson M, Genheden S, Diehl C, Qvist J, Weininger U, Nilsson UJ, Leffler H, Ryde U, Akke M et al. 2012. The carbohydrate-binding site in galectin-3 is preorganized to recognize a sugarlike framework of oxygens: Ultra-high-resolution structures and water dynamics. *Biochemistry*. 51:296–306.

Sato S, Hughes RC. 1992. Binding specificity of a baby hamster kidney lectin for H type I and II chains, polylactosamine glycans, and appropriately glycosylated forms of laminin and fibronectin. *J Biol Chem*. 267:6983–6990.

Sauerzapfe B, Krenek K, Schmiedel J, Wakarchuk WW, Pelantova H, Kren V, Elling L. 2009. Chemo-enzymatic synthesis of poly-*N*-acetyllactosamine (poly-LacNAc) structures and their characterization for CGL2-galectin-mediated binding of ECM glycoproteins to biomaterial surfaces. *Glycoconj J*. 26:141–159.

Shekhar MPV, Nangia-Makker P, Tait L, Miller F, Raz A. 2004. Alterations in galectin-3 expression and distribution correlate with breast cancer progression: Functional analysis of galectin-3 in breast epithelial-endothefial interactions. *Am J Pathol*. 165:1931–1941.

Song XZ, Xia BY, Stowell SR, Lasanajak Y, Smith DF, Cummings RD. 2009. Novel fluorescent glycan microarray strategy reveals ligands for galectins. *Chem Biol*. 16:36–47.

Stanley P. 2014. Galectin-1 pulls the strings on VEGFR2. *Cell*. 156:625–626.

Stowell SR, Arthur CM, Mehta P, Slanina KA, Blixt O, Leffler H, Smith DF, Cummings RD. 2008. Galectin-1, -2, and -3 exhibit differential recognition of sialylated glycans and blood group antigens. *J Biol Chem*. 283: 10109–10123.

Vijayakumar S, Peng H, Schwartz GJ. 2013. Galectin-3 mediates oligomerization of secreted hensin using its carbohydrate-recognition domain. *Am J Physiol-Renal*. 305:F90–F99.

von Mach T, Carlsson MC, Straube T, Nilsson U, Leffler H, Jacob R. 2014. Ligand binding and complex formation of galectin-3 is modulated by pH variations. *Biochem J*. 457:107–115.

Wang Y, Nangia-Makker P, Tait L, Balan V, Hogan V, Pienta KJ, Raz A. 2009. Regulation of prostate cancer progression by galectin-3. *Am J Pathol*. 174:1515–1523.

Yamaoka A, Kuwabara I, Frigeri LG, Liu FT. 1995. A human lectin, galectin-3 (epsilon bp/Mac-2), stimulates superoxide production by neutrophils. *J Immunol*. 154:3479–3487.

Yang RY, Hill PN, Hsu DK, Liu FT. 1998. Role of the carboxyl-terminal lectin domain in self-association of galectin-3. *Biochemistry*. 37:4086–4092.

Yegorova S, Chavaroche AE, Rodriguez MC, Minond D, Cudic M. 2013. Development of an AlphaScreen assay for discovery of inhibitors of low-affinity glycan-lectin interactions. *Anal Biochem*. 439:123–131.